Available online at www.sciencedirect.com
ScienceDirect
C. R. Physique 7 (2006) 1000–1017
COMPTES RENDUS PHYSIQUE
http://france.elsevier.com/direct/COMREN/

Nucleation/Nucléation

Cavitation in water: a review

Frédéric Caupin *, Eric Herbert

Laboratoire de Physique Statistique de l'École Normale Supérieure, associé aux Universités Paris 6 et 7 et au CNRS, 24, rue Lhomond, 75231 Paris cedex 05, France

Abstract

Liquid water can be brought beyond the liquid–vapor equilibrium line into a metastable state, before nucleation of bubbles (cavitation) occurs. We review the experimental work on cavitation in water, focusing on the determination of the ultimate degree of metastability at which liquid water can exist. We also present practical applications of metastability and cavitation. ***To cite this article: F. Caupin, E. Herbert, C. R. Physique 7 (2006).***

Résumé

Cavitation dans l'eau : revue. L'eau liquide peut être amenée au-delà de la ligne d'équilibre liquide–vapeur jusque dans un état métastable, avant que la nucléation de bulles (cavitation) n'intervienne. Nous passons en revue les travaux expérimentaux sur la cavitation dans l'eau, en mettant l'accent sur la détermination du degré de métastabilité extrême auquel l'eau liquide peut exister. Nous présentons également des applications pratiques de la métastabilité et de la cavitation. ***Pour citer cet article : F. Caupin, E. Herbert, C. R. Physique 7 (2006).***

Keywords: Water; Metastability; Superheated liquid; Stretched liquid; Cavitation

Mots-clés : Eau ; Métastabilité ; Liquide surchauffé ; Liquide sous tension ; Cavitation

1. Introduction

Any liquid can be prepared in a metastable state with respect to its vapor in two ways: either by superheating above its boiling temperature T_b, or by stretching below its saturated vapor pressure P_{sat}. It will eventually return to equilibrium by nucleation of vapor bubbles (cavitation). This phenomenon is of fundamental interest for our understanding of first order transitions.

Reviews are available that focus on different aspects: superheated liquids [1], stretched liquids [2], both [3], and metastable liquids in general [4]; other references are more particularly devoted to bubble formation and dynamics in acoustic cavitation [5,6], hydrodynamic cavitation [7] or both [8]. Here, we will focus on water and try to bring the information up-to-date. In water, the interest is increased because of the relation to water structure, and also in view of the practical aspects. We first give a brief overview of the theoretical background about cavitation and the

* Corresponding author.
E-mail address: caupin@lps.ens.fr (F. Caupin).

1631-0705/$ – see front matter
doi:10.1016/j.crhy.2006.10.015

peculiar case of water (Section 2). In Sections 3 and 4, we review the numerous experimental methods that have been used to study cavitation in water, focusing on the maximum degree of metastability achievable in ultrapure water, but also leaving room for historical aspects. A strong disagreement is found between different experiments, and between experiments and theory; we investigate in Section 5 the possible explanations. In Section 6, we address the role of walls and impurities (heterogeneous cavitation). Finally, in Section 7, we present practical aspects and applications of metastable liquid water and cavitation.

2. Theoretical background

We begin with a theoretical introduction to homogeneous nucleation, that is the birth of the new phase due to thermal fluctuations of the system. We keep the discussion to the minimum required to discuss the experimental results, and refer the reader to Refs. [4,9,10] for more details.

2.1. Nucleation theory

Classical nucleation theory (CNT) has been developed in several works (see the references given in Ref. [4]). A simple version (e.g. [11]) will help us to understand the origin of metastability. Let us consider a liquid superheated at constant pressure P to a temperature T above T_b, or, equivalently, stretched at constant temperature T to a pressure P below $P_{sat}(T)$. The minimum work required to create a sphere of vapor of radius R in the liquid is

$$\frac{4}{3}\pi R^3(P - P') + 4\pi R^2\sigma \tag{1}$$

where P' is the pressure at which the vapor is at the same chemical potential as the liquid at P (see [12] for example), and σ is the liquid–vapor surface tension. Far from the critical point, $P' - P \simeq P_{sat}(T) - P$. The first term in Eq. (1) gives the energy gained when forming a volume of the stable phase, whereas the second term is the energy cost associated with the creation of an interface. Their competition results in an energy barrier

$$E_b = \frac{16\pi}{3}\frac{\sigma^3}{(P' - P)^2} \tag{2}$$

reached for a critical bubble of radius $R_c = 2\sigma/(P' - P)$. Nucleation occurs at a rate proportional to $\exp[-E_b/(k_bT)]$: it will be likely when E_b becomes comparable to the thermal fluctuations. A more detailed study (e.g. [13]) shows that the probability to cavitate reaches $1/2$ when

$$\frac{E_b}{k_bT} = \ln\left(\frac{\Gamma_0 V\tau}{\ln 2}\right) \tag{3}$$

where V and τ are the volume and duration of the experiment considered. Γ_0 is a kinetic prefactor, which can be estimated as the product of a thermal frequency k_bT/h and a density of independent nucleation sites $1/R_c^3$ [13] (other choices are possible, e.g. Ref. [11]). The logarithmic dependence in Eq. (3) has two consequences: Γ_0 has not to be known accurately, and experiments with very different $V\tau$ will have nearly the same theoretical cavitation temperature T_{cav} or pressure P_{cav}. Fig. 1 shows the prediction of CNT for water. Water is a strongly cohesive liquid, because of hydrogen bonding between its molecules. This makes σ unusually high, and theoretically allows a high degree of metastability. For instance, with $V = (10\ \mu m)^3$ and $\tau = 1$ s, $T_{cav} = 306\ ^\circ C$ at atmospheric pressure. At this temperature, the equilibrium P_{sat} is 9.3 MPa: one can also describe the system as in a stretched state; temperature and pressure are equivalent parameters controlling the departure from equilibrium.

An important comment should be made at this point: pressure in a metastable liquid can become negative, as reveals the inspection of the low temperature region of Fig. 1. For instance, with the above values of $V\tau$, CNT predicts $P_{cav} = -168$ MPa at 20 °C. This surprising statement becomes more reasonable if one thinks in terms of density: a negative pressure corresponds to a liquid density reduced compared to the equilibrium one. The molecules in the liquid are then further away from each other, but their mutual attraction allows the system to remain metastable. This, however, cannot hold for any density: for too large intermolecular distances, the system becomes mechanically unstable. This critical density is called the spinodal density ρ_s, corresponding to a spinodal pressure P_s: at this point the compressibility of the metastable liquid diverges ($(\partial P/\partial V)_T$ vanishes), and long wavelength perturbations can

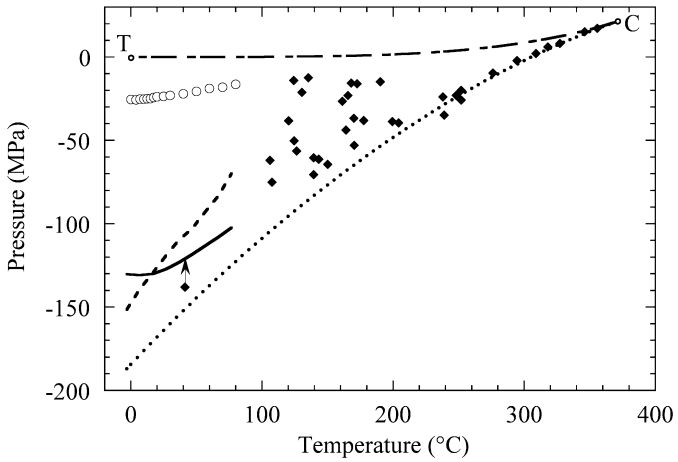

Fig. 1. Cavitation pressure in water as a function of temperature, calculated with CNT [15] (dotted line), or using DFT with Speedy's EOS [16] (solid line) or with the EOS from a recent MDS [20] (short-dashed line). The parameters used are $V = (10\,\mu\text{m})^3$, $\tau = 1$ s, and Γ_0 given in the text. The dash-dotted line shows the saturated vapor pressure from the triple point (T) to the critical point (C). Some experimental results are also shown. Filled diamonds correspond to experiments on mineral inclusions [76]; the arrow shows a correction to the pressure estimate (see Section 4.4). Empty circles are our data obtained with an acoustic method [92] (see Section 4.7).

grow without limit [4]. The spinodal parameters may be estimated by extrapolation of the equation of state (EOS) measured at positive pressure (see Section 2.2).

As the liquid becomes unstable at the spinodal, the barrier for cavitation E_b should vanish: this feature is missing in CNT. To take it into account, one resorts to density functional theory (DFT), details of which can be found elsewhere [9,14,15]. DFT includes the EOS of the fluid, and allows one to search for critical nuclei with a smooth variation of the density, whereas CNT deals only with vapor bubbles separated from the liquid by a sharp jump in density. Therefore DFT always finds a lower E_b, which vanishes at P_s, as required.

2.2. The spinodal of water

In this paragraph we consider specifically the spinodal of water. As we shall see, its behavior may be different from that of other liquids. We also discuss the theoretical predictions for the homogeneous cavitation line $P_{cav}(T)$.

As $(\partial P/\partial V)_T = 0$ at P_s, the simplest analytic expression of the EOS close to the spinodal would be:

$$P(V,T) = P_s(T)\left[1 - B\left(\frac{V_s(T)}{V} - 1\right)^2\right] \tag{4}$$

Speedy found that the EOS for water, measured in the range 0–100 °C and 0–100 MPa, was very well fitted by this simple formula [16]. Interestingly, he found that $P_s(T)$ had a minimum of −212 MPa around 30 °C. Speedy was able to relate this to the fact that water possesses a line of density maxima (LDM): it shrinks upon heating below 4 °C at atmospheric pressure. If the LDM meets the spinodal $P_s(T)$, the latter is bound by thermodynamics to change slope [16]; the minimum of $P_s(T)$ found in Speedy's fit with Eq. (4) indeed occurs at a temperature where the linear extrapolation of the LDM reaches the spinodal. Only a few liquids exhibit a LDM: helium 3 is among them, and theoretical and experimental evidence was found for such a spinodal with a minimum [17].

Later on, competing EOSs have been proposed based on molecular dynamics simulations (MDS) with several intermolecular potentials [18–20]. They all find a monotonic $P_s(T)$; they remain thermodynamically consistent because they find at the same time that the LDM retraces to lower temperature without ever reaching the spinodal. The debate on the spinodal of water is part of a fundamental debate on the anomalies of supercooled water (when the liquid is metastable compared to the solid). We refer the reader to Refs. [4,21] for a recent review.

Now, as DFT uses the EOS as an input, it is interesting to compare the predictions for P_{cav} for different EOSs. This is done in Fig. 1: interestingly, the absence or presence of a minimum in $P_s(T)$ is found to be reflected in $P_{cav}(T)$ [15]. This is encouraging, because, $P_{cav}(T)$ can be reached and directly measured in experiments, whereas $P_s(T)$ cannot. We will now review the experimental results on $P_{cav}(T)$. Of course, the answer to the question about the minimum

in $P_s(T)$ lies at low temperature and negative pressure. However, for the sake of comprehensiveness, our review will cover all temperatures, up to the critical point.

3. Superheated water

We have chosen to describe separately the many different experimental methods used to study cavitation in water. We are mainly interested in the highest degree of metastability observed, but we also give a brief historical survey. As noted above, any state of the liquid beyond the liquid–vapor equilibrium is metastable. However, for convenience, we give in this section the results obtained by heating the liquid above T_b; we postpone the review of experiments where the pressure is lowered below P_{sat} to Section 4.

3.1. Heating in a capillary

This method consists in heating a vessel filled with water by immersion in a hot bath. De Luc was the first to report about superheated water at the end of the 18th century (he cites his experiment in Ref. [22]): using a glass flask in an oil bath, he could heat water purged of air to 122.5 °C at atmospheric pressure without boiling. Donny [23] used a glass tube, 8 mm in diameter, heated inside boiling calcium chloride solutions with different concentrations. For water purged of air by boiling before testing, he found $T_{cav} = 135$ °C at atmospheric pressure. To minimize the effect of impurities, and to allow a quick thermalization, small capillaries are used; an oil bath is preferred for its reduced evaporation. Kenrick et al. [24] used boiled pure water in small (0.3 to 1 mm inner diameter) Pyrex capillaries, and found that vapor explosion occurred at a maximum $T_{cav} = 270$ °C; this was later confirmed by Briggs [25]. More recently, Brereton et al. [26] used distilled water, degassed under vacuum, pre-compressed at 100 MPa and transferred in silica capillaries. The open capillary was heated by 5 °C steps and then inspected by light microscopy. Bubbles were detected at 240 °C (resp. 170 °C) in 20 μm (resp. 150 μm) diameter capillaries.

3.2. Heating in a host liquid

Droplets of water can be heated in another liquid with higher T_b. The interest of this method is two-fold: it involves a smooth liquid–liquid interface, and the volume of liquid can be made small. In 1861, Dufour [27] used a mixture of linseed oil and clove spirit to match water density; he observed that 1–2 mm floating droplets could be heated up to 178 °C before cavitation occurred. A development of this method is the bubble column: a droplet of the liquid studied is injected at the bottom of a column of a denser host liquid, where a temperature gradient is maintained. The droplet raises slowly and warms up above T_b, until it cavitates at some height where T_{cav} is measured. It was first devised by Moore [28] and Wakeshima et al. [29]. For water heated in silicone oil at atmospheric pressure, T_{cav} lies in the range 250–280 °C [30,31], but the mutual solubility between the liquids is not negligible at this high temperature. Replacing silicone oil with benzyl benzoate which is less soluble, Apfel achieved a maximum T_{cav} of 279.5 °C [32].

3.3. Heat pulse

The liquid can also be directly heated by a thin platinum wire. A large current is passed through the heater for a short time (typically 10 μs). When a bubble nucleates, it reduces the heat transfer to the fluid, and the heater temperature raises. The corresponding change in resistance of the wire allows one to detect cavitation; preliminary calibration of the resistance gives T_{cav}. Skripov and his group have used this method to measure T_{cav} at different static pressures [33]; at atmospheric pressure they obtained $T_{cav} = 302$ °C [34]. This value is close to the prediction of CNT for homogeneous nucleation (see Fig. 2), and was later confirmed by Derewnicki [35] and Glod et al. [36], who found $T_{cav} = 292$ and 303 °C, respectively (the accuracy in T_{cav} is estimated to be ±5 °C [36]).

This method has been recently revisited by a number of groups using a thin film heater instead of a wire. The maximum values of T_{cav} are similar. Specifically: 296 °C [37], 283 °C [38], 300 °C [39], and 296 °C [40]; the uncertainty may however be larger than for the wire experiments, because of possibly larger thermal gradients along the heater. Note also that the thin film heater was made of platinum, except in Ref. [38] where it was a proprietary alloy (Ta–Al) used in commercial thermal ink jet printers (see Section 7.3). We shall come back to this method to discuss heterogeneous cavitation (Section 6) and applications (Section 7.3).

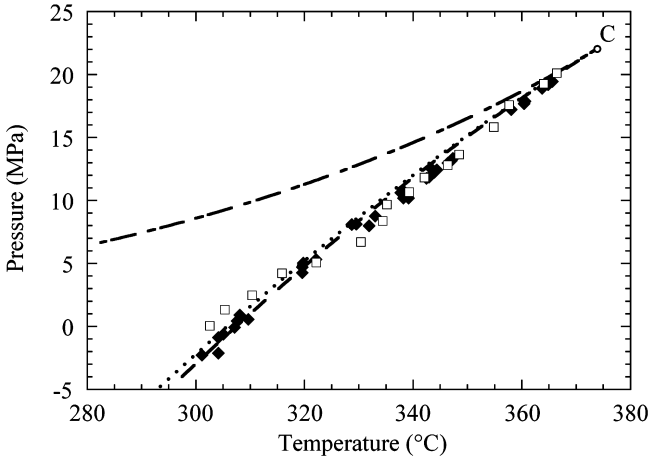

Fig. 2. Cavitation pressure in water as a function of temperature. The empty squares were obtained with the pulse heating method [33] (see Section 3.3), the filled diamonds with mineral inclusions [76] (see Section 4.4). The dash-dotted line shows the saturated vapor pressure up to the critical point (C). The dotted (resp. dashed) line is the prediction of CNT (see Section 2) for Γ_0 given in the text and the parameters relevant for the inclusions (resp. pulse heating experiments): $V = (10\ \mu\text{m})^3$, $\tau = 1$ s (resp. $V = (100\ \mu\text{m})^3$, $\tau = 1\ \mu$s). Despite the large change in $\Gamma V \tau$, the two curves lie close to each other.

3.4. Laser induced cavitation

Water can be heated by illumination with light at a wavelength which is absorbed. CO_2 lasers have been used to warm up small size droplets [41,42] or the surface of a liquid water bath [43]. It was found that vapor explosion of the droplet occurs only above a threshold in the laser fluence [42,43]. Using the experimental threshold, T_{cav} was estimated to be above 300 °C [42,43]; however, the calculation relies on a number of assumptions (on the heat absorption) that limit its accuracy.

Yavas et al. [44] used an indirect method: a 16 ns excimer laser pulse (at 248 nm, where water is transparent) is absorbed by a thin (200 nm) chromium film (1 cm × 1 cm) immersed in the liquid. A probe laser measures the reflectivity of the film, which drops when a bubble is nucleated. Again, there is a threshold fluence for cavitation, which can be used to estimate T_{cav} by simulation of heat diffusion in the system: they find 153 °C. The simulations have been confirmed experimentally by measuring the reflectance of a thin film optical temperature sensor placed under the chromium film [45]. However, Yavas et al. later noticed that T_{cav} was detector dependent: heating water with a 25 ns pulse on a 53 nm silver film (1 cm × 1 cm), the reflectivity method gives $T_{\text{cav}} = 200$ °C, whereas a more sensitive surface plasmon probe (SPP) used simultaneously gives a lower threshold: $T_{\text{cav}} = 111$ °C [46]. The difference is interpreted with the help of a simulation of the spatial temperature profile in water. An upper bound for the bubble size is given by the thickness of the superheated layer: 20 and 90 nm at the SPP and reflectivity threshold, respectively [46]. These numbers would correspond to the minimum size of the bubbles detectable by each method. These findings put the heat pulse work into question: is it possible that the detection technique is not sensitive enough, and overestimates T_{cav}? The heat pulse experiments involve a much smaller heater area than laser heating (60 × 60 μm versus 1 cm × 1 cm), so that the laser heating experiments are more sensitive to heterogeneous nucleation. On the other hand the SPP used with laser heating probes only a small area of the heated film (the cross section of the He–Ne probe beam). Another factor is the time scale of the heat pulse: 20 ns and 10 μs for the laser and heat pulse experiments, respectively: one can expect that the superheated layer will be thicker in the latter, allowing the bubbles to grow enough to be detected by the usual methods (see Section 3.3) as soon as the nucleation threshold is reached. It would be interesting to use the SPP in a heat pulse experiment to settle this issue.

4. Stretched water

We continue the review of cavitation experiments with methods where the pressure of the liquid is lowered below P_{sat}.

4.1. Pull

A straightforward way to stretch a liquid is to pull directly on it. The pull can be generated by the own weight of the liquid. This is how Huygens made the first experimental observation of negative pressure in 1662, and published his work in 1672 [49]. A tube open at one end is filled with water purged of air, and inverted over a water bath. If the air above the bath is evacuated, water remains suspended in the inverted tube. The pressure at the top of the water column of height h is $P_{\mathrm{sat}} - \rho g h$, where ρ is water density, and g the acceleration of gravity. As soon as a bubble of air is injected in the tube, it rises and the water column falls. This experiment was presented to the Royal Society of England, and repeated on water and mercury by several physicists, including the famous Hooke and Boyle, who reached -0.2 MPa in mercury. The phenomenon was later re-discovered by Donny [23] and Reynolds [47,48]. Details are given by Kell [50]. As Reynolds used a 2.3 m-long tube wetted with water before being filled with mercury, he obtained the most negative pressure for water with this method: -0.3 MPa [48]. Hayward, who thought that the method was invented by Donny [23], re-used it to study different liquids [51].

Another way to pull a liquid is to mechanically increase its volume with a bellow for instance. One can also put the liquid under pressure before warming it up, and eventually releasing the pressure. These techniques have been widely used to make bubble chambers where high energy particles are detected because they trigger cavitation in the metastable liquid (see Ref. [53] for a review); however, volatile liquids with a low surface tension were preferred to water. But the bellow method was used by Hayward to design a water pump with a suction lift of 17 m, corresponding to a pressure of -0.17 MPa [52]; much higher liquid columns exist in tall trees (see Section 7.1).

4.2. Hydrodynamic flow

For a horizontal, inviscid steady flow, with a velocity distribution v, the Bernoulli equation tells that $P + \rho v^2$ is constant along a streamline. Thus the pressure is reduced in the region of high flow. Using glass Venturi tubes (that is tubes with a constriction), Reynolds was the first to show that this effect can lead to bubble nucleation [54]; he also recognized that the bubbles appear close to the saturated vapor pressure because of the air occluded in water. In fact, this technique has been adapted to characterize the distribution of cavitation nuclei in water channels [7]: the flow through a Venturi tube is progressively increased, leading to the explosion of nuclei with more and more negative thresholds, and allowing to measure their distribution. Heterogeneous cavitation in a flow is of practical importance (see Section 7.5). On the other hand, we are not aware of hydrodynamic experiments having reached large values of P_{cav}.

4.3. Berthelot method

In this section we review a method used over more than 150 years, and named after its inventor, Marcellin Berthelot [55]. In view of their conceptual interest, we shall also describe experiments on other liquids than water and on other properties than the cavitation pressure.

The Berthelot method consists in the following. A vessel is filled with liquid and sealed. If a gas bubble remains, the setup is warmed up until the bubble dissolves completely; from the dissolution temperature T_{d}, the liquid density is deduced. The vessel is then cooled down, the liquid sticks to its walls and the pressure decreases, down to negative pressure if the temperature is low enough. At some temperature T_{cav}, cavitation occurs and the liquid goes back to equilibrium with its vapor. Berthelot estimated the volume change of the liquid upon cavitation by measuring the size of the bubble formed; from the isothermal compressibility χ_{T} of the liquid, he deduced the corresponding $P_{\mathrm{cav}} = \Delta V/\chi_{\mathrm{T}}$. Another way to obtain P_{cav} is to convert the difference between T_{d} and T_{cav} into a pressure change by

$$\Delta P = P_{\mathrm{d}} - P_{\mathrm{cav}} = \int_{T_{\mathrm{cav}}}^{T_{\mathrm{d}}} \frac{\alpha_{\mathrm{P}}}{\chi_{\mathrm{T}}}\,\mathrm{d}T \tag{5}$$

where α_{P} is the isobaric expansion coefficient and P_{d} the pressure in the tube at T_{d}, usually neglected. In Eq. (5) the value of χ_{T} measured at positive pressure is usually used, although χ_{T} in the stretched liquid may be different. This can be accounted for by using an EOS extrapolated to negative pressures (see Section 4.4). Corrections may be made for the thermal expansion of the vessel. Based on the bubble volume, Berthelot achieved $P_{\mathrm{cav}} = -5$ MPa at 18 °C [55],

and Dixon and Joly −0.7 MPa (in the presence of wood chips, see Section 7.1) [56]. Later, based on Eq. (5), Dixon obtained −16 MPa at 72.9 °C [57] and Vincent −15.9 MPa at 54 °C [58,59].

However, the assumption that P_d is negligible has been criticized [59–65]. The problem is that to dissolve the last air bubble in a reasonable time, high pressures have to be reached inside the tube. Lewis [64] could measure this pressure to be 6.8 MPa for one tube. In this case, P_{cav} is less negative than thought. Several attempts have been made to check this. Vincent and Simmonds [59] studied mineral oil. Following the usual method, they obtained $P_{cav} = -12$ MPa; when sealing the tube by freezing the liquid near its exit, to make sure that $P_d = 0.1$ MPa, they obtained at most −2.5 MPa. The subsequent experiments were made on water. Temperley and Chambers measured the change in volume of the water just before (the pressure is then near P_{cav}) and after (the pressure is then near zero) cavitation by a weighing method [60]; P_{cav} was down to −6.8 MPa, and less negative than using Eq. (5) with $P_d = 0$. The Berthelot method can be adapted to have a direct estimate of P_{cav}, without any assumption about P_d (see below). Several groups thus obtained P_{cav} down to −4.2 MPa [61], −5 MPa [64], and −2 MPa [65] respectively; the measured values of P_{cav} were systematically less negative than that calculated from Eq. (5). Scott et al. [63] used Eq. (5), neglecting P_d, but sealed the tubes without any air: they obtained P_{cav} down to −5.6 MPa. All these experiments noticed a large scatter of P_{cav} between tubes or between runs with the same tube.

Clearly, a direct measurement of P_{cav} is necessary to make the method reliable. The first modification of the Berthelot method in this direction is due to Worthington [66]. A bulb filled with mercury, and provided with a narrow graduated capillary, was enclosed in a Berthelot tube. It served as a tonometer: when the liquid was under tension, it made the bulb expand by a volume measured from the change of the mercury level in the capillary. The system was calibrated by applying positive pressures on the bulb; a linear extrapolation gave the negative pressure exerted by the stretched liquid. In addition, the Berthelot tube ended with another capillary, in which cavitation could be triggered (by briefly heating a platinum wire) and the volume of the vapor bubble measured. Worthington was thus able to measure the EOS of the liquid (pressure-volume relation) at negative pressure. He only studied ethanol, and found that the pressure and volume were linearly related in the range from −1.7 to +1.2 MPa (with the temperature varying between 11 and 21 °C). Part of this method was later [61,64,65] adapted in the following way: the Berthelot tube was now surrounded by a water-jacket ending with a capillary open to the atmosphere. When cavitation occurs, the tube expands by a volume measured with the capillary, and P_{cav} is calculated from the elasticity of the tube.

Another way to measure P_{cav} is to shape the glass capillary serving as a Berthelot tube into an helix to make a Bourdon gauge. The change in internal pressure makes the helix coil or uncoil, and the rotation is measured with a mirror attached to it [67–69] or a capacitance distance meter [70]. As for Worthington's method, the system is calibrated at positive pressure and the calibration extrapolated to negative pressure. Meyer studied water, ethanol and ether, obtaining $P_{cav} = -3.4$ MPa at 24 °C, −3.95 MPa at 23 °C, and −7.3 MPa at 18 °C, respectively [67]. He measured the pressure-volume relation, and found it to be linear, except for ether where he noticed a curvature. He also measured the LDM of water and found it to lie near the linear extrapolation of positive pressure measurements. Evans measured P_{cav} in the range from −3 to −5 MPa, between 35 and 20 °C [70]. Henderson and Speedy found cavitation at −16 MPa at 38 °C [68]. They also extended the work of Meyer on the LDM down to −20.3 MPa at 8.3 °C [69]. They could reach lower values of P_{cav} than in previous experiments because of the smaller volume of water involved and the cleanliness of their system.

These latter methods to measure P_{cav} are expected to be quite accurate, because the extrapolation of the calibration relies only on the linear elasticity of the glass, not on an assumption about the properties of the stretched liquid. Finally, one can use an electrical strain gauge pressure transducer. This was done in Trevena's group with stainless steel Berthelot tubes: they first obtained P_{cav} down to −0.19 MPa [71], and could reach −4.7 MPa by first evacuating air from the tube before filling with boiled distilled water [72]. The latter procedure was used in Ohde's group, who automated the experiments to repeat thousands of thermal cycles, reaching a minimum P_{cav} of −18.5 MPa at 53 °C [73].

4.4. Quartz inclusions

Water trapped in small pockets (in the 10–100 μm range) inside crystals can be found in nature. Roedder [74] used such microscopic inclusions to prepare ice crystals and liquid water in metastable equilibrium. He started with liquid and vapor in the inclusion. Upon freezing, the vapor disappears because of the greater volume of ice. When

the inclusion is melted again, if the vapor does not nucleate, a negative pressure develops as the system follows the metastable melting line. A maximum ice–liquid equilibrium temperature of 6.5 °C was observed; by an extrapolation of the melting line measured at positive pressure, Roedder estimated the corresponding pressure to be at least −90 MPa.

Angell and his group used the Berthelot method in synthetic inclusions [75,76]. As their first paper deals with inclusions of saline solutions [75], we will focus on the second one where Raman spectra of the inclusions indicated a low salt concentration [76]. Crystals (quartz, calcite and fluorite) are quench-fissured in pure water between 300 and 400 °C. The fractured crystals are then sealed in Ag–Pd tubes with a known amount of ultrapure water, and autoclaved. During autoclaving, healing of the fissures traps water in inclusions at a desired density, depending on the autoclaving temperature and pressure. Angell and his group then followed Berthelot method to study these inclusions: the bubble remaining in the inclusion disappears upon heating, at a temperature T_d; when the sample is cooled down, liquid water follows a nearly isochoric path, until cavitation occurs at T_{cav}. To deduce P_{cav}, they have to rely on an EOS: they chose to extrapolate the so-called Haar–Gallagher–Kell (HGK) EOS to negative pressure. The HGK EOS is a multiparameter EOS fitted on data measured at pressures where the liquid is stable; it is qualitatively similar to Speedy EOS, but quantitatively different, giving for the coordinates of the minimum in the spinodal around 60 °C and −160 MPa.

For quartz inclusions, all inclusions in a given sample have the same T_d and hence the same density. There are two distinct cavitation behaviors. When $T_d > 250$ °C (autoclaving temperature higher than 400 °C), T_{cav} is the same within ±2 °C for all inclusions in a given sample. At low enough density, P_{cav} is positive, and the results agree well with the superheating experiments discussed above (see Section 3 and Fig. 2). On the other hand, when $T_d < 250$ °C (high density inclusions), T_{cav} is scattered. For fluorite and calcite, T_{cav} is always scattered, and the estimated P_{cav} is less negative than in quartz. Angell and his group attribute the scatter to heterogeneous nucleation, and its source to "*possibly surfactant molecules cluster destroyed by annealing at the higher temperatures*". The maximum tension is obtained in one sample with high density inclusions (0.91 g mL^{-1} and $T_d = 160$ °C); Angell and his group report that "*some [inclusions] could be cooled to −40 °C without cavitation, and one was observed in repeated runs to nucleate randomly in the range 40 to 47 °C and occasionally not at all*" [76]: they estimate that nucleation occurred at $P_{cav} \simeq -140$ MPa. The fact that "*no inclusion that survived cooling to 40 °C ever nucleated bubbles during cooling to lower temperatures*" was interpreted as an evidence that the isochore crosses the metastable LDM, thus retracing to less negative pressure at low temperature. This gives support to Speedy's scenario, at least in the sense that the LDM keeps a negative slope, deep in the negative pressure region in the P–T plane.

Further work on inclusions deals with the use of Brillouin scattering to measure the sound velocity in stretched liquid water [77]. This study reports tensions beyond −100 MPa at 20 °C. In addition, it was able to show a volume change in a platelet-like inclusion, which points out the difficulty with the isochoric assumption made to estimate P_{cav}; on the other hand, for roughly spherical inclusions this assumption appears to be appropriate. It should be emphasized that in the work by Angell and his group, the inclusions in which they estimated $P_{cav} \simeq -140$ MPa "*were not of well-rounded form, like those on which the reliable and reproducible high temperature data were obtained*" [78]. To conclude with mineral inclusions, we shall mention a recent work focusing on kinetic aspects, by measuring the statistics of lifetimes of one inclusion at fixed temperatures [79]. The largest negative pressure achieved in this work is −16.7 MPa at 258.3 °C, and the lifetimes follow a Poisson distribution, as expected theoretically.

4.5. Centrifugation

This method, first employed by Reynolds [80], consists in rotating at high speed a tube containing water. Because of the centrifugal force, a negative pressure is developed on the rotation axis: $P = P_0 - \frac{1}{2}\rho\omega^2 r^2$ where P_0 is the pressure outside the tube, ρ is the water density, and r is the distance between the center and the liquid–gas interface. The first studies achieved a minimum value for P_{cav} of −0.49 MPa [80] and −0.57 MPa [60]. The most negative P_{cav} was obtained by Briggs [81] with boiled distilled water in Pyrex capillaries (0.6–0.8 mm inner diameter). Briggs also investigated the temperature variation of P_{cav}: he found a minimum of −27.7 MPa at 10 °C, with $P_{cav} = -2$ MPa at 0 °C and −22 MPa at 50 °C. Later quartz tubes were used [82]; P_{cav} was found to be scattered between tubes and to vary with time in the same tube, reaching at best −17.5 MPa.

4.6. Shock waves

A review of the techniques involving shock waves is given in Ref. [2]. The negative pressure can be generated directly by the tube arrest technique: a tube filled with water is sent upward by springs and is suddenly stopped. It can also be generated by reflection of a positive pressure pulse at the interface between water and a medium with lower acoustic impedance (e.g. air); the initial positive pulse may be generated by an underwater explosion or by the bullet–piston method (the steel bottom of a water tube is stricken by a bullet). Finally, the water shock tube experiments generate the tensile pulse either directly (the pressure of the gas above the liquid is suddenly released) or by reflection (combustion above the liquid generates a compressional wave which travels down and back, before being reflected at the free surface). At the time Ref. [2] was written, the bullet–piston method with a stainless steel tube gave the most negative P_{cav} (measured with a piezoelectric transducer), -1.47 MPa [83]; in addition, a minimum of $P_{\mathrm{cav}}(T)$ was found at 5 °C, similarly to Briggs [81], but at less negative pressures. Since then, it was further investigated and lead to -9 MPa [84]. In a similar impact technique, the pressure was deduced by interferometric velocity measurement of a Mylar diaphragm; the most negative pressures reached were -11.5 MPa [85] and -10.2 MPa [86].

The experiment by Wurster et al. [87] is of particular interest. A weakly focused shock wave generated by an electromagnetic generator is further focused by reflection on a parabolic reflector. A fiber optic probe hydrophone measures the reflectivity of a laser beam at the fiber/water interface, from which the density of the liquid is deduced; the pressure is then estimated thanks to an extrapolation of Tait equation of state for water [88]. With a rigid reflector, they find cavitation at -27 MPa on the hydrophone surface. On the other hand, with a soft reflector, they were able to reach "*−59 MPa without cavitation at the fiber tip*". They claim that "*the reason for this is that the adhesion of water to clean glass is higher than the cohesion of water itself*"; in fact, cavitation actually occurs away from the fiber tip [89]. As the study does not report any threshold for the onset of cavitation away from the tip, we will use the value -27 MPa for comparison (see Section 5), keeping in mind that this technique seems able to prepare liquid water at large negative pressures, at least close to the fiber tip.

4.7. Acoustic cavitation

An acoustic wave can quench liquid water to negative pressure (during its negative swing). Standing and travelling waves, focused or not, were used by countless different groups. Most of the experiments observed cavitation at very moderate negative pressures ($+0.1$ MPa $> P_{\mathrm{cav}} > -1$ MPa), because of the presence of cavitation nuclei (see Section 6) in the experimental volume. We will restrict the present discussion to the experiments that reached the most negative pressures [90–92].

Galloway [90] used a standing wave produced by a spherical resonator. The sound amplitude at the center is measured with a piezoelectric microphone. Galloway defines the threshold for cavitation as the point "*at which cavitation will occur at least once a minute, while a 10 percent reduction in the peak sound pressure will not produce any cavitation in a 15-minute interval*". He found that P_{cav} at 22 °C varies from -0.1 MPa for distilled water saturated with air, to -20 MPa for distilled water degassed at 0.02% saturation. The way to define the threshold is of fundamental importance, because Galloway states that "*pressure 100 times greater than this threshold pressure may be imposed on the sample for short lengths of time, of the order of seconds, without causing cavitation*"; we also learn from Finch [93] that Galloway [94] "*generally obtained much lower thresholds, of the order of 15–20 atm [−1.5−−2 MPa], with the higher values [−20 MPa] occurring only at certain times, there being no obvious explanation for the change*". Contrarily to Briggs [81], Galloway noticed a small monotonic increase of P_{cav} with temperature (10% between 5 and 45 °C). Greenspan and Tschiegg [91] used a standing wave focused in a cylinder made of stainless steel to study carefully cleaned and degassed water. They calibrated P_{cav} by the static pressure method: the static pressure of the liquid (the pressure when the sound is off) is increased, and the driving voltage of the system has to be increased accordingly to reach P_{cav}. By extrapolating linearly the variation measured between 0 and 0.8 MPa to zero voltage, they found $P_{\mathrm{cav}} = -16$ MPa (resp. -21 MPa) at 30 °C for an average waiting time for cavitation of several minutes (resp. seconds).

In our experiment [92], we use a few cycles of a 1 MHz travelling wave, tightly focused at the center of an hemispherical piezoelectric transducer immersed in the liquid; the experimental volume is 2.1×10^{-4} mm^3. The liquid is subjected to a high negative pressure during a short time (the effective experimental time is 45 ns), and cavitation occurs when the amplitude is sufficient. We measure the probability Σ of this random phenomenon by

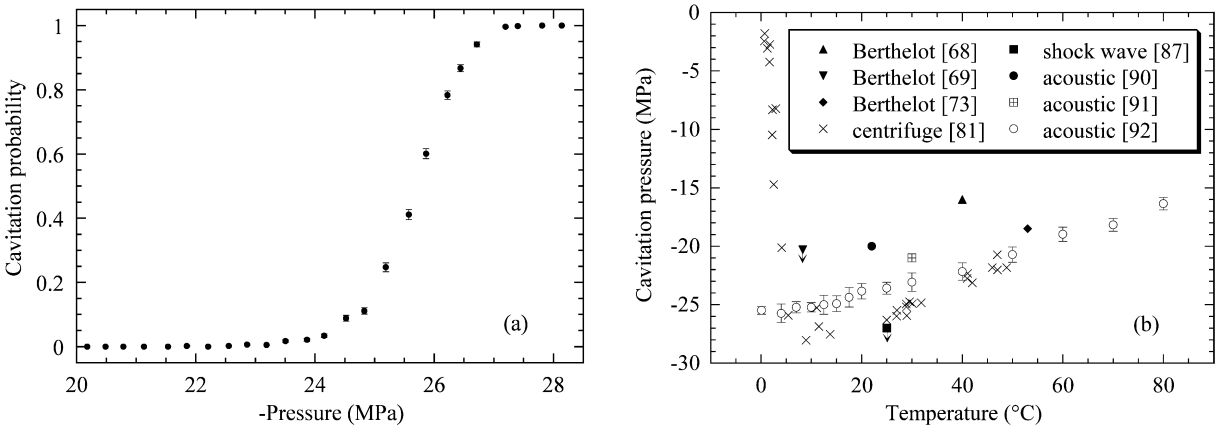

Fig. 3. (a) Cavitation probability as a function of pressure at 4 °C. Each data point was obtained by repeating 1000 acoustic bursts. The error bars are calculated from the binomial law. (b) Cavitation pressure as a function of temperature for different experiments: the corresponding method and reference are given in the legend. Only the experiments with the most negative cavitation pressures were selected, except the inclusion work, for sake of clarity. An arrow means that cavitation was not observed. The error bars on the empty circles represent the uncertainty on the pressure calibration.

repeating the sound bursts for a given amplitude. The high reproducibility of our experimental setup allows us to measure a probability-amplitude curve (Fig. 3(a)) with better accuracy than in previous experiments, with Σ going from 0 to 1 in a narrow pressure range. This is expected because of the strong exponential dependence of Σ on $E_b(P)$ (see Section 2.1) and provides a clear definition of the cavitation threshold P_{cav}, at which $\Sigma = 0.5$. The pressure is calibrated by two methods: the first uses a commercial needle hydrophone; the second is the static pressure method of Greenspan and Tschiegg ([91], see above), but extended to higher static pressure around 9 MPa, which gives more accuracy. The two methods agree well and give P_{cav} from -26 MPa at 0 °C to -17 MPa at 80 °C.

5. Discussion

Comparison of the available data on cavitation in water leads to the following statements. At high temperature (specifically in the superheated liquid region at positive pressure, see Section 3), different experimental techniques find close values of T_{cav}, in good agreement with theoretical expectations. The situation is strikingly different at low temperature (in the stretched liquid region at negative pressure, see Section 4). Among the countless cavitation experiments, only the ones with special care about water purity can reach large negative pressures; with a variety of techniques, they all obtain P_{cav} around -25 MPa at room temperature (see Fig. 3 (b)), which falls far away from the theoretical value (from -120 to -140 MPa). There is a notable exception: experiments with mineral inclusions achieve -140 MPa. The large gap between these data requires special attention.

First, one could question the cleanliness of experiments other than the inclusion ones. However, it is surprising that different techniques lead to very close values of P_{cav}. One could think that the nature of the wall plays a role: water adhesion may be stronger on the quartz walls of the inclusions. However, we note that some acoustic experiments found $\simeq -20$ MPa in the absence of walls, and that Strube and Lauterborn [82], using the centrifugation method with quartz tubes, reached at best -17.5 MPa. We must then turn to dissolved or floating impurities. In our experiment, great care was taken to work with the purest samples. Ultrapure water was degassed and transferred under vacuum in the experimental setup, made of materials which do not affect water quality [92]. We have checked the reproducibility of our results, with time in the same sample, between different samples of the same ultrapure water supply, and between water samples of different origin. On the other hand, in the inclusion case, the cavitation pressures are much more scattered at low temperature than at high temperature, with -140 MPa reported only for one inclusion. This behavior was attributed to impurities ("*possibly surfactant molecule clusters*"): most of them would be destroyed by the high temperature annealing involved in the making of the inclusions, but a small concentration would remain, of the order of one impurity by inclusion. The volumes of the inclusions are around $(10\ \mu m)^3$, smaller than the experimental volume in our setup (around $(60\ \mu m)^3$), which could explain the discrepancy. However, because of the high reproducibility of our results and the sharp cavitation threshold we find, such impurities would have to be

ubiquitous and amazingly calibrated. Detailed analysis of the cavitation statistics [92] rules out the possibility of 'mechanical' impurities like gas bubbles trapped on hydrophobic particles (see Section 6.2). The only remaining possibility would be a type of impurity lowering the energy barrier for cavitation; but again the same impurity is required to explain all the experimental results. One could think about cosmic rays which would trigger cavitation, but they are not relevant for the small length and time scales involved, their typical total flux at sea level being only $240\,\mathrm{m}^{-2}\,\mathrm{s}^{-1}$ [95].

An alternative explanation lies in the reliability of the pressure calibration. In several of the non inclusion experiments (Berthelot or Berthelot–Bourdon, centrifuge, acoustic), P_{cav} is directly measured. On the other hand, the inclusion experiments measure the cavitation *temperature*. The pressure is then deduced using an EOS measured at positive pressure and extrapolated in the negative pressure region; this is questionable, even if the order of magnitude of the pressure reached is consistent with the EOS from molecular dynamics simulations. A possibility would be that the extrapolation is wrong, so that the actual P_{cav} is closer to the one obtained in experiments not using inclusions. This would make the experiments consistent with each other, but not with the theory. But if the extrapolated EOS is wrong, the spinodal deduced from the extrapolation is wrong also. In our acoustic experiment, if cavitation is homogeneous, the accurate cavitation statistics allows one to calculate the new spinodal pressure (see [92] for details): in this picture, P_{s} would have to be around -50 MPa instead of -200 MPa. Two attempts have been made to measure the EOS at negative pressure. Meyer [67] measured the pressure-volume (P–V) relation down to -3.4 MPa with a Berthelot method (see Section 4.3), and found it consistent with a linear extrapolation from positive pressures. An attempt was made to use centrifugation (see Section 4.3) to check the EOS [96]. A tube containing water being rotated, the angular velocity and the meniscus position are measured; from this one deduces the specific volume of the liquid, averaged over the pressure range developed along the liquid column (down to -10 MPa). However, the analysis has been criticized [97] and reconsidered [98,99]. The average makes it difficult to fully determine the P–V curve. If its curvature is set to zero, a small systematic deviation between the calculated slope and the one accurately measured at positive pressure is found [99]; on the other hand, if its slope is fixed to the positive pressure value, and the data reanalyzed to give the curvature, the value obtained is five times greater than in the positive region [99]. This is a weak support of our hypothesis about an unexpectedly low negative value of P_{s}.

The picture of cavitation in water is still not complete. Two directions can be investigated to settle the debate. On one hand, even more efforts should be made to purify the water sample; one could also reduce the experimental volume (by increasing the frequency of the acoustic experiment for instance) to be less sensitive to impurities. On the other hand, a definite measurement of the EOS at negative pressure is needed; this requires the simultaneous measurement of two independent thermodynamical quantities. We plan to use optical techniques to get the local and instantaneous density and sound velocity inside the sound wave used for acoustic cavitation.

6. Heterogeneous cavitation

It is a challenging task to obtain homogeneous nucleation: only the best experiments have been described above; many others find cavitation at a very small degree of metastability (e.g. a few atmospheres in many acoustic experiments). Most often, cavitation will be heterogeneous, occurring on impurities that lower the threshold for nucleation. In order to better understand the results of some experiments, we now give a short discussion of some mechanisms of heterogeneous nucleation: on flat hydrophobic surfaces (Section 6.1) and on pre-existing bubbles (Section 6.2).

6.1. Surfaces

In some of the methods described above, the metastable liquid is in contact with a solid substrate. Depending on its wetting properties, it may lower the energy needed to create a vapor bubble. Let σ, σ_{SV} and σ_{SL} be the liquid–vapor, solid–vapor and solid–liquid surface tension, respectively. Volmer [100] has shown that, on a smooth substrate,

$$E_{\mathrm{b}} = \frac{16\pi}{3}\,\frac{\sigma^3}{(P'-P)^2}\,\frac{(2-\cos\theta)(1+\cos\theta)^2}{4} \tag{6}$$

where θ is the equilibrium contact angle of water on the surface, $\cos\theta = (\sigma_{\mathrm{SV}} - \sigma_{\mathrm{SL}})/\sigma$. The effect becomes important only for large enough θ; e.g., for $\theta = 53°$, E_{b} is reduced by 10% compared to homogeneous cavitation (Eq. (2)).

One could think of varying the wetting properties of the surface to check this. In a heat pulse experiment [39] (see Section 3.3), a gold plated platinum film was used to heat water: T_{cav} was 274 °C on this hydrophilic surface. The heater was then coated with hydrophilic or hydrophobic self-assembled monolayer (SAM). On hydrophilic SAMs, T_{cav} lies between 270 and 284 °C, whereas on hydrophobic SAMs, T_{cav} falls as low as 197 °C. For hydrophobic SAMs, T_{cav} increases when the heat pulses are repeated, and lies between 259 and 274 °C after 1000 pulses; this is attributed to a progressive desorption of the SAMs, exposing the bare gold substrate. These observations are consistent with the fact that the contact angle of water is larger on the hydrophobic than on the hydrophilic SAMs (even if, strictly speaking, this angle has been measured at room temperature, not near T_{cav}). However, the idealized case of a smooth substrate may not reflect the experimental situation. We shall see in the next paragraph how the roughness of the substrate plays a role in cavitation. In Ref. [39], the substrate appears smooth on a 100 nm scale, but could have defects of smaller size.

Nevertheless, an ideally smooth substrate can be obtained with the test liquid immersed in a host liquid. This is relevant for the bubble column method (see Section 3.2). Three types of nucleation are then possible: usual cavitation inside the test liquid, vapor of the test liquid forming in the host liquid (bubble blowing), or cavitation at the liquid–liquid interface. In the third case, as the substrate is now deformable, Eq. (6) has to be modified. For the nucleation in a liquid A in contact with a liquid B, one finds [30]

$$E_{\mathrm{b}} = \frac{16\pi}{3}\frac{1}{(P-P_{\mathrm{sat}})^2}\left[\frac{1}{2}(\sigma_{\mathrm{A}}^3+\sigma_{\mathrm{B}}^3)+\frac{1}{16}\sigma_{\mathrm{AB}}^3+\frac{3}{8}\frac{\sigma_{\mathrm{A}}^2\sigma_{\mathrm{B}}^2}{\sigma_{\mathrm{AB}}}-\frac{3}{8}\sigma_{\mathrm{AB}}\left(\sigma_{\mathrm{A}}^2+\sigma_{\mathrm{B}}^2\right)-\frac{3}{16}\frac{\sigma_{\mathrm{A}}^4+\sigma_{\mathrm{B}}^4}{\sigma_{\mathrm{AB}}}\right] \tag{7}$$

where σ_{A}, σ_{B} and σ_{AB} are the liquid A–A vapor, liquid B–A vapor, and liquid A-liquid B surface tension, respectively. For water heated in a silicone oil, Apfel [30] predicted $T_{\mathrm{cav}} = 286$ °C instead of 298 °C for homogeneous nucleation, and found at most 269 °C experimentally. The bubble blowing mechanism has been reported for water superheated in a fluorinated ether [101]: T_{cav} was in the range 218–228 °C, to compare to the predicted value, 233 °C. However, the values of the parameters in Eq. (7) are uncertain: in particular, σ_{AB} has to be extrapolated from measurements at low temperature. In both experiments, the solubility between water and the host liquid was not negligible at high temperature: this may affect T_{cav}. Using benzyl benzoate, which is less soluble in water than silicone oil, gives $T_{\mathrm{cav}} =$ 279.5 °C [32], closer to the homogeneous value.

6.2. Pre-existing bubbles

Heterogeneous nucleation may occur on pre-existing bubbles. Free floating bubbles are unlikely: they are seen to raise or dissolve rapidly [102], as expected theoretically [103]. To act as cavitation nuclei, they should be stabilized in some way.

The crevice model was proposed to explain the stability and to calculate the cavitation threshold of trapped bubbles; it was later refined by several authors (see Ref. [104] and references therein). Consider an air bubble inside a conical pit in a surface that water does not wet. If the pressure in the bubble P_{in} is higher than P_{diss}, the pressure required for equilibrium with the air dissolved in the water (Henry's law), air will diffuse into solution, and the bubble will shrink. Eventually the contact angle with the wall reaches the advancing contact angle of the contact line, and the bubble then shrinks towards the apex of the cone. The system reaches equilibrium when $P_{\mathrm{in}} = P_{\mathrm{diss}}$, which occurs when the interface has a radius of curvature $R = (P_{\mathrm{w}} - P_{\mathrm{diss}})/(2\sigma)$, where P_{w} is the pressure in liquid water (Laplace's law). Now if P_{w} is released, the bubble starts growing: first the interface changes curvature, and if the contact angle reaches the receding angle of the contact line, it moves away from the apex of the cone, reaches a macroscopic size and leads to cavitation (see however Ref. [104] for corrections to this model).

It has been noticed that pre-pressurizing the liquid allows higher degrees of metastability to be reached [105]. The crevice model explains this by the fact that the application of positive pressure forces the trapped bubble to the bottom of the pit, until its disappearance if the pressure is sufficiently high. Pulse heating experiments (see Section 3.3) have shown that T_{cav} increased with increasing heating rate, reaching a saturation value close to the theoretical homogeneous T_{cav} [36]. This is consistent with the crevice model. Trapped bubbles need some time to grow out of the cracks. At low heating rates this effect dominates and prevents further heating of the liquid, whereas at high heating rates one is able to heat the liquid close to the homogeneous limit.

Another mechanism of bubble stabilization was proposed by Fox and Herzfeld [106], and later reconsidered by Yount [107]: gas bubbles would be covered by an organic skin. The skin would limit gas diffusion into solution; its

tearing strength would determine the cavitation threshold, and its crumbling strength would explain the high pressurization needed to destroy the nuclei. In fact such nuclei can be manufactured and used to seed water, with applications in medicine (see Section 7.2). Nevertheless, even if Yount et al. claimed to have seen natural occurrence of such nuclei [107], we believe that gas bubbles trapped on cracks are a more frequent source of heterogeneous cavitation.

It is interesting to look experimentally for the effect of controlled bubble nuclei. Recently, Bremond et al. [108,109] used an acoustic wave to create bubbles on a hydrophobic (silanized) silicon wafer. On a smooth substrate (roughness less than 2 nm) freshly immersed in water, bubbles nucleate at low negative pressure ($P > -4$ MPa) on preferential sites for nucleation. This is attributed to trapped gas: cavitation does not occur if a thin ethanol film is left on the surface of the wafer before immersion. The density of sites decreases with time (because of gas diffusion) and with repeated cavitation (because gas is exhausted from the traps). The situation can be controlled if the wafer is patterned with cylindrical cavities (15 μm deep and 4 μm diameter): cavitation occurs reproducibly on gas pockets entrapped on these defects, provided that the sample is pulled off the water and plunged again to refill the cavities between acoustic shots. This setup also allows the study of the interaction between bubbles whose positions and distances are controlled and decoupled from their radial motion.

Trapped bubbles provide an ubiquitous source of nuclei that can be invoked to explain many experimental observations. However, they are not sufficient to resolve the discrepancy between the recent acoustic cavitation and the inclusion results (see Section 5). In the acoustic experiment, focusing allows one to study cavitation in a small volume of liquid away from the container walls. The probability-pressure curves (see Section 5 and Fig. 3(a)) are reproducible and well described by a model of thermally activated nucleation [92]. One would need a large concentration of floating solid particles with well calibrated cracks to explain these observations; furthermore, the absence of dependence of the cavitation statistics on the ultrasonic frequency excludes nuclei with a threshold due to mechanical instability [92]. If cavitation is heterogeneous in our experiment, we have to find another kind of impurity, which lowers the energy barrier for nucleation. One can think of some dissolved molecule, that disrupts the hydrogen bond network of liquid water and favors vapor formation; but no clear picture is available at present.

7. Practical aspects

Water is ubiquitous, being at the same time the most abundant liquid on earth, the fluid of life, and a very good solvent. It is therefore not surprising to find cavitation in water involved in many different contexts, with either positive or adverse effects. It is beyond the reach of this review to make a comprehensive list; we can just point out some areas in which cavitation is an important phenomenon. For each of them, we will attempt to give a flavor of the physical process involved, and refer the reader to topical reviews and recent literature.

7.1. Water in nature

The law of hydrostatics teaches us that the pressure drop in a water column of 10.2 m is 0.1 MPa. This points out that negative pressures can be reached in the ascending sap of tall trees. In fact additional effects (viscous flow, drought) make the pressure in the sap negative even at smaller heights. The cohesion-tension theory, first proposed by Dixon and Jolly [56], explains that the sap column is held at the top by the meniscus in the pore of the leaves: by Laplace's law, the meniscus curvature allows a pressure jump between the outside air pressure and the negative pressure in the sap. The trees thus contain large amounts of metastable liquids. Cavitation may sometimes occur, disrupting the liquid column and stopping the flow (xylem emboly). The complex hydraulic architecture of trees limits the damage, and strategies exist to refill the embolied xylem channels. Much work has been devoted to this topic, and is reviewed in Refs. [110,111].

Another example of cavitation in nature is given by some shrimps. By the fast closing of an appendage, they can generate cavitation and use it to communicate or stun preys [112–114].

7.2. Medicine

Ultrasound is widely used in medicine, and there has been a long standing debate about its possible unwanted bio-effects (reviewed for example by Leighton [5, Chapter 5.4.2]). Absorption of sound can locally heat tissues (this is actually used to destroy tumors), and cavitation may occur and induce damage.

Extracorporeal shock wave lithotripsy, used to destroy kidney or gall stones, involves a high amplitude shock wave produced outside the body, and focused through the tissues on the stones. The mechanism for stone fragmentation is still debated, and, in addition to the transient stresses exerted by the shock, cavitation may play a role (Ref. [5, Chapter 5.4.2 (iv)]).

Ultrasonic contrast agents are used in medical imaging. They are made of gas bubbles stabilized with a coating shell (phospholipid, surfactant, albumin or polymer). The acoustic impedance mismatch with the blood in which they are injected makes them strong scatterers of the acoustic wave, useful to check blood perfusion in organs, or to measure blood flow rate by Doppler velocimetry for instance. The concern with their use arises because they are known to lower the threshold for cavitation, and studies are aimed at determining the possible bio-effects, and the acoustic power up to which they may be safely used.

On the other hand, the potential of microbubbles to cavitate is currently investigated to design novel imaging methods or therapeutic applications [115]. In imaging, for example, microbubbles can be destroyed locally by cavitation, and the time necessary for their renewal will give information on the perfusion status. The bubbles may be targeted to attach preferentially to selected cells, which can then be detected by cavitation imaging. For therapy, cavitation of microbubbles is proposed to destroy clots in veins (sonothrombolysis), or to allow a temporary opening of the blood brain barrier without damage to the neurons, to enable delivery of molecules to the brain. Microbubbles may also incorporate drugs or genes (in the interior of the bubbles, or embedded in the coating, or also attached to the outside); cavitation is then triggered by ultrasound at a specific site for localized drug or gene delivery.

7.3. Ink jet printers

The central element of a thermal ink-jet printer is a microheater actuator. A thin film resistor (typically a square of 60×60 μm) is heated in a short time (typically less than 5 μs), and nucleates boiling of the ink on its surface. The bubble expands and pushes the liquid into a nozzle, eventually ejecting a drop at the nozzle exit. This process can be repeated with a high rate, around 20 kHz, to print on paper. This setup has been used by several groups to study the limit of superheat of water (see Section 3.3). It is better to use short and powerful heat pulses to get closer to the homogeneous cavitation temperature [36,38]; this is important to release the highest mechanical power in the liquid, as shown by Glod et al. [36] (using a platinum wire as the heater). Recently, high-speed imaging techniques were used to visualize the microboiling at the 10 ns timescale [40,116,117]. New applications of this technology of microbubble production are actively studied, from printing polymer electronics to making pumps in microfluidics (see references given in Ref. [117]).

7.4. Vapor explosions

When a cold liquid, normally boiling at a temperature T_b, comes into contact with another liquid hotter than T_b, the former can become superheated. Cavitation may suddenly occur, and the large increase in volume due to vapor formation lead to violent explosions [1]. In the case of hydrocarbons and water, cavitation occurs in the liquid hydrocarbon. But cavitation in water may be responsible for explosions in accidental spills of molten metals. Another example is provided by volcanoes: water superheated by magma can lead to destructive explosions [118].

On the other hand, microscopic vapor explosions can be used to improve the combustion of fuel [119–122]. Water and fuel are mixed to form an emulsion, with the help of surfactants. For some hydrocarbons and in a certain range of water content, the phenomenon of microexplosion occurs. During combustion of a droplet, water or fuel inside the emulsion becomes superheated, until cavitation occurs, atomizing the droplet into fine secondary droplets, increasing the mixing with air. The potential benefit of this technique is to improve the combustion efficiency, reduce the formation of soot, particulate matter, unburned hydrocarbons, and carbon monoxide.

7.5. Cavitation damage

It is well known that screw propellers of ships induce cavitation which causes a reduction of thrust and damage on the propeller blades. Erosion and damage by cavitation are clearly reviewed in Refs. [5, Chapter 5.4.1] or [7]. We will just mention here that damage arises during the cavity collapse, by two mechanisms. First, the collapse emits a large shock wave in the liquid, whose effects can be enhanced by the collective collapse of many bubbles in a cavitation

cloud. The second mechanism is due to asymmetric collapse: because of the proximity of a wall, or of a passing shock wave (emitted by another collapsing bubble), the bubble loses its spherical shape, a high speed liquid jet is formed and impinges the solid surface.

The violent collapse of cavitation bubbles may also prove useful, as in cleaning or lithotripsy (see Section 7.2). Ultrasonic cleaning is a common example. More recently, steam laser cleaning has been developed. A thin liquid film is deposited on the surface to be cleaned, and rapidly heated by a pulsed laser. The explosive boiling of the liquid is able to remove particles down to 0.2 μm. The nucleation begins at small superheating, but it is more efficient when a higher surface temperature is reached, allowing bubbles to grow to a larger size [46].

7.6. Sonochemistry

The term sonochemistry covers the effects of ultrasound on chemical reactions. They were first reported in 1927, but sonochemistry really became a widely studied branch of chemistry in the 1980s. A review can be found in Ref. [123] for example. The underlying mechanism of sonochemistry is cavitation. Reactions involving solid surfaces as reagents or catalysts are improved by the mechanical effects associated with the collapse of a bubble: cleansing of and oxide removal from the surface (see Section 7.5) enhance its reactivity, and molecules are efficiently swept over the surface. But in a homogeneous liquid phase, cavitation has also chemical effects. The most commonly accepted mechanism is the same as for sonoluminescence (see Ref. [5, Chapter 5.2]): during the bubble collapse, high temperature and pressure are reached, able to generate highly reactive radical species. Sonochemistry increases the rate and yields of many chemical reactions, and sometimes allow to change the nature of the products. Ref. [124] provides a recent survey of organic synthesis by sonochemistry. Ref. [125] gives examples of synthesis of nanoparticles and microspheres used in medicine (see Section 7.2). Decontamination is another application of sonochemistry [123]: cavitation is used to kill microorganisms (when combined with chlorine) and to destroy organic pollutants in water.

8. Conclusion

Stretched and superheated water has been studied for more than 240 years. To observe the metastable states and measure the cavitation threshold, numerous techniques have been used. The wide scatter of the results emphasizes the role of walls and impurities in the onset of cavitation. Conditions of extreme purity are necessary to obtain homogeneous nucleation. The disagreement between experiments and theory for the limiting negative pressure that can be reached raises fundamental questions about the equation of state of water. On the other hand, practical aspects rather involve lower level of purity. They cover a wide range of natural phenomena, and medical or industrial applications. The understanding of the underlying mechanism for heterogeneous nucleation is required to be able to predict, avoid or trigger cavitation.

Acknowledgements

We thank S. Balibar for helpful discussions, and J.-M. Allain, E. Katzav, P. Leiderer, and Y. Poncel for their help with the bibliography. Support from ANR Grant No. 05-BLAN-0084-01 and Grant No. JC05-48942 is acknowledged.

References

[1] R.C. Reid, Superheated liquids, Amer. Sci. 64 (1976) 146–156.
[2] D.H. Trevena, Cavitation and Tension in Liquids, Adam Hilger, Bristol, Philadelphia, 1987.
[3] C.T. Avedisian, The homogeneous nucleation limits of liquids, J. Phys. Chem. Ref. Data 14 (1985) 695–729.
[4] P.G. Debenedetti, Metastable Liquids, Princeton Univ. Press, Princeton, NJ, 1996.
[5] T.G. Leighton, The Acoustic Bubble, Academic Press, London, 1994.
[6] C.E. Brennen, Cavitation and Bubble Dynamics, Oxford Univ. Press, New York, 1995, also available at http://resolver.caltech.edu/CaltechBOOK:1995.001.
[7] J.-P. Franc, J.-M. Michel, Fundamentals of Cavitation, Kluwer Academic Publishers, Dordrecht, Boston, London, 2004.
[8] F.R. Young, Cavitation, Imperial College Press, London, 1999.
[9] D.W. Oxtoby, Homogeneous nucleation: theory and experiment, J. Phys.: Condens. Matter 4 (1992) 7627–7650.
[10] H.J. Maris, Theory of nucleation, C. R. Physique, this issue, DOI: 10.1016/j.crhy.2006.10.019.
[11] J.C. Fisher, The fracture of liquids, J. Appl. Phys. 19 (1948) 1062–1067.

[12] S. Balibar, F. Caupin, Nucleation of crystals from their liquid phase, C. R. Physique, DOI:10.1016/j.crhy.2006.10.024.
[13] M.S. Pettersen, S. Balibar, H.J. Maris, Experimental investigation of cavitation in superfluid ^{4}He, Phys. Rev. B 49 (1994) 12062–12070.
[14] J.W. Cahn, J.E. Hilliard, Free energy of a nonuniform system. III. Nucleation in a two-component incompressible fluid, J. Chem. Phys. 31 (1959) 688–699.
[15] F. Caupin, Liquid–vapor interface, cavitation, and the phase diagram of water, Phys. Rev. E 71 (1–5) (2005) 051605.
[16] R.J. Speedy, Stability-limit conjecture. An interpretation of the properties of water, J. Phys. Chem. 86 (1982) 982–991.
[17] F. Caupin, S. Balibar, H.J. Maris, Anomaly in the stability limit of liquid helium 3, Phys. Rev. Lett. 87 (2001) 145302 (1–4).
[18] P.H. Poole, F. Sciortino, U. Essmann, H.E. Stanley, Spinodal of liquid water, Phys. Rev. E 48 (1993) 3799–3817.
[19] P.A. Netz, F.W. Starr, H.E. Stanley, M.C. Barbosa, Static and dynamic properties of stretched water, J. Chem. Phys. 115 (2001) 344–348.
[20] M. Yamada, S. Mossa, H.E. Stanley, F. Sciortino, Interplay between time–temperature transformation and the liquid–liquid phase transition in water, Phys. Rev. Lett. 88 (2002) 195701 (1–4).
[21] P.G. Debenedetti, Supercooled and glassy water, J. Phys.: Condens. Matter 15 (2003) R1669–R1726.
[22] J.-A. De Luc, Introduction à la physique terrestre par les fluides expansibles, Paris, 1803, p. 93.
[23] F. Donny, Mémoire sur la cohésion des liquides, et sur leur adhérence aux corps solides, Ann. Chim. Phys. 16 (1846) 167–190.
[24] F.B. Kenrick, C.S. Gilbert, K.L. Wismer, The superheating of liquids, J. Phys. Chem. 28 (1924) 1297–1307.
[25] L.J. Briggs, Maximum superheating of water as a measure of negative pressure, J. Appl. Phys. 26 (1955) 1001–1003.
[26] G.J. Brereton, R.J. Crilly, J.R. Spears, Nucleation in small capillary tubes, Chem. Phys. 230 (1998) 253–265.
[27] M.L. Dufour, Sur l'ébullition des liquides, C. R. Acad. Sci. 52 (1861) 986–989;
M.L. Dufour, Sur l'ébullition des liquides, C. R. Acad. Sci. 53 (1861) 846–849.
[28] G.R. Moore, Vaporization of superheated drops in liquids, AIChE J. 5 (1959) 458–466.
[29] H. Wakeshima, K. Takata, On the limit of superheat, J. Phys. Soc. Japan 13 (1958) 1398–1403.
[30] R.E. Apfel, Vapor nucleation at a liquid–liquid interface, J. Chem. Phys. 54 (1971) 62–63.
[31] M. Blander, D. Hengstenberg, J.L. Katz, Bubble nucleation in *n*-pentane, *n*-hexane, *n*-pentane + hexadecane mixtures, and water, J. Phys. Chem. 75 (1971) 3613–3619.
[32] R.E. Apfel, Water superheated to 279.5 °C at atmospheric pressure, Nature Phys. Sci. 238 (1972) 63–64.
[33] P.A. Pavlov, V.P. Skripov, Kinetics of spontaneous nucleation in strongly heated liquids, High Temp. (USSR) 8 (1970) 540–545; translated from Teplofiz. Vys. Temp. 8 (1970) 579–585.
[34] V.P. Skripov, P.A. Pavlov, Explosive boiling of liquids and fluctuation nucleus formation, High Temp. (USSR) 8 (1970) 782–787; translated from Teplofiz. Vys. Temp. 8 (1970) 833–839.
[35] K.P. Derewnicki, Experimental studies of heat transfer and vapour formation in fast transient boiling, Int. J. Heat. Mass Trans. 28 (1985) 2085–2092.
[36] S. Glod, D. Poulikakos, Z. Zhao, G. Yadigaroglu, An investigation of microscale explosive vaporization of water on an ultrathin Pt wire, Int. J. Heat. Mass Trans. 45 (2002) 367–379.
[37] Y. Iida, K. Okuyama, K. Sakurai, Boiling nucleation on a very small film heater subjected to extremely rapid heating, Int. J. Heat. Mass Trans. 37 (1994) 2771–2780.
[38] C.T. Avedisian, W.S. Osborne, F.D. McLeod, C.M. Curley, Measuring bubble nucleation temperature on the surface of a rapidly heated thermal ink-jet heater immersed in a pool of water, Proc. R. Soc. London A 455 (1999) 3875–3899.
[39] O.C. Thomas, R.E. Cavicchi, M.J. Tarlov, Effect of surface wettability on fast transient microboiling behavior, Langmuir 19 (2003) 6168–6177.
[40] K. Okuyama, S. Tsukahara, N. Morita, Y. Iida, Transient behavior of boiling bubbles generated on the small heater of a thermal ink jet printhead, Exp. Therm. Fluid Sci. 28 (2004) 825–834.
[41] P. Kafalas, A.P. Ferdinand Jr., Fog droplet vaporization and fragmentation by a 10.6-μm laser pulse, Appl. Opt. 12 (1973) 29–33.
[42] R.G. Pinnick, A. Biswas, R.L. Armstrong, S.G. Jennings, J.D. Pendleton, G. Fernandez, Micron-sized droplets irradiated with a pulsed CO_2 laser: measurement of explosion and breakdown thresholds, Appl. Opt. 29 (1990) 918–925.
[43] S.I. Kudryashov, K. Lyon, S.D. Allen, Photoacoustic study of relaxation dynamics in multibubble systems in laser-superheated water, Phys. Rev. E 73 (2006) 055301(R) (1–4).
[44] O. Yavas, P. Leiderer, H.K. Park, C.P. Grigoropoulos, C.C. Poon, W.P. Leung, N. Do, A.C. Tam, Optical reflectance and scattering studies of nucleation and growth of bubbles at a liquid–solid interface induced by pulsed laser heating, Phys. Rev. Lett. 70 (1993) 1830–1833.
[45] H.K. Park, C.P. Grigoropoulos, C.C. Poon, A.C. Tam, Optical probing of the temperature transients during pulsed–laser induced boiling of liquids, Appl. Phys. Lett. 68 (1996) (1993) 596–598.
[46] O. Yavas, A. Schilling, J. Bischof, J. Boneberg, P. Leiderer, Bubble nucleation and pressure generation during laser cleaning of surfaces, Appl. Phys. A 64 (1997) 331–339.
[47] O. Reynolds, On the internal cohesion of liquids and the suspension of a column of mercury to a height more than double that of the barometer (1877), in: Scientific Papers on Mechanical and Physical Subject, vol. I, Cambridge Univ. Press, Cambridge, 1900–1903, pp. 231–243 (Chapter 31).
[48] O. Reynolds, Some further experiments on the cohesion of water and mercury (1880–81), in: Scientific Papers on Mechanical and Physical Subject, vol. I, Cambridge Univ. Press, Cambridge, 1900–1903, pp. 394–398 (Chapter 35).
[49] C. Huygens, Extrait d'une lettre de M. Hugens de l'Académie Royale des Sciences à l'auteur de ce journal, touchant les phénomènes de l'eau purgée d'air, J. des Sçavants, 25 juillet 1672; partial English translation: Phil. Trans. 7 (1672) 5027–5030.
[50] G.S. Kell, Early observations of negative pressures in liquids, Am. J. Phys. 51 (1983) 1038–1041.
[51] A.T.J. Hayward, The role of stabilized gas nuclei in hydrodynamic cavitation inception, J. Phys. D 3 (1970) 574–579.
[52] A.T.J. Hayward, Mechanical pump with a suction lift of 17 metres, Nature 225 (1970) 376–377.

[53] R.P. Shutt (Ed.), Bubble and Spark Chambers: Principles and Use, Academic Press, New York, London, 1967.
[54] O. Reynolds, Experiments showing the boiling of water in an open tube at ordinary temperatures (1894), in: Scientific Papers on Mechanical and Physical Subject, vol. II, Cambridge Univ. Press, Cambridge, 1900–1903, pp. 578–587 (Chapter 63).
[55] M. Berthelot, Sur quelques phénomènes de dilatation forcée des liquides, Ann. Chim. Phys. 30 (1850) 232–237.
[56] H.H. Dixon, J. Joly, On the ascent of sap, Phil. Trans. Roy. Soc. B 186 (1895) 563–576.
[57] H.H. Dixon, Note on the tensile strength of water, Sci. Proc. Roy. Dublin Soc. 12 (1909) 60–65.
[58] R.S. Vincent, Measurement of tension in liquids by means of a metal bellows, Proc. Roy. Soc. 53 (1941) 126–140.
[59] R.S. Vincent, G.H. Simmonds, Examination of the Berthelot method to study tension in liquids, Proc. Roy. Soc. 55 (1943) 376–382.
[60] H.N.V. Temperley, LL.G. Chambers, The behaviour of water under hydrostatic tension: I, Proc. Phys. Soc. 58 (1946) 420–436.
[61] H.N.V. Temperley, The behaviour of water under hydrostatic tension: II, Proc. Phys. Soc. 58 (1946) 436–443.
[62] H.N.V. Temperley, The behaviour of water under hydrostatic tension: III, Proc. Phys. Soc. 59 (1947) 199–208.
[63] A.F. Scott, D.P. Shoemaker, K.N. Tanner, J.G. Wendel, Study of the Berthelot method for determining the tensile strength of a liquid, J. Chem. Phys. 16 (1948) 495–502.
[64] G.M. Lewis, The tensile strength of liquids in Berthelot tubes, Proc. Phys. Soc. 78 (1961) 133–144.
[65] E.P. Rees, D.H. Trevena, A study of the Berthelot method of measuring tensions in liquids, Brit. J. Appl. Phys. 17 (1966) (1961) 671–674.
[66] A.M. Worthington, On the mechanical stretching of liquids: an experimental determination of the volume-extensibility of ethyl alcohol, Phil. Trans. Roy. Soc. A 183 (1892) 355–370.
[67] J. Meyer, Zur Kenntnis des negativen Druckes in Flüssigkeiten, Abhandl. d. Deutsch. Bunsen–Gessellschaft 6 (1911) 1–53.
[68] S.J. Henderson, R.J. Speedy, A Berthelot–Bourdon tube method for studying water under tension, J. Phys. E: Sci. Instrum. 13 (1980) 778–782.
[69] S.J. Henderson, R.J. Speedy, Temperature of maximum density in water at negative pressure, J. Phys. Chem. 91 (1987) 3062–3068.
[70] A. Evans, A transparent recording Berthelot tensiometer, J. Phys. E: Sci. Instrum. 12 (1979) 276–281.
[71] P.J. Chapman, B.E. Richards, D.H. Trevena, Monitoring the growth of tension in a liquid contained in a Berthelot tube, J. Phys. E: Sci. Instrum. 8 (1975) 731–735.
[72] W.M. Jones, G.D.N. Overton, D.H. Trevena, Tensile strength experiments with water using a new type of Berthelot tube, J. Phys. D: Appl. Phys. 14 (1981) 1283–1291.
[73] K. Hiro, Y. Ohde, Y. Tanzawa, Stagnations of increasing trends in negative pressure with repeated cavitation in water/metal Berthelot tubes as a result of mechanical sealing, J. Phys. D: Appl. Phys. 36 (2003) 592–597.
[74] E. Roedder, Metastable superheated ice in liquid–water inclusions under high negative pressure, Science 155 (1967) 1413–1417.
[75] J.L. Green, D.J. Durben, G.H. Wolf, C.A. Angell, Water and solutions at negative pressure: Raman spectroscopic study to −80 megapascals, Science 249 (1990) 649–652.
[76] Q. Zheng, D.J. Durben, G.H. Wolf, C.A. Angell, Liquids at large negative pressures: water at the homogeneous nucleation limit, Science 254 (1991) 829–832.
[77] A.D. Alvarenga, M. Grimsditch, R.J. Bodnar, Elastic properties of water under negative pressures, J. Chem. Phys. 98 (1993) 8392–8396.
[78] Q. Zheng, J. Green, J. Kieffer, P.H. Poole, J. Shao, G.H. Wolf, C.A. Angell, Limiting tensions for liquids and glasses from laboratory and MD studies, in: A.R. Imre, H.J. Maris, P.R. Williams (Eds.), Proceedings of the NATO Advanced Research Workshop on Liquids Under Negative Pressure, Budapest, 2002, in: NATO Science Series, Series II: Mathematics, Physics and Chemistry, vol. 84, Kluwer, Dordrecht, 2002, pp. 33–46.
[79] M. Takahashi, E. Izawa, J. Etou, T. Ohtani, Kinetic characteristic of bubble nucleation in superheated water using fluid inclusions, J. Phys. Soc. Japan 71 (2002) 2174–2177.
[80] O. Reynolds, cited in Ref. [66].
[81] L.J. Briggs, Limiting negative pressure of water, J. Appl. Phys. 21 (1950) 721–722.
[82] H.W. Strube, W. Lauterborn, Untersuchung der Kavitationskeime an der Grenzfläche Quarzglas–Wasser nach der Zentrifugenmethode, Z. Angew. Phys. 29 (1970) 349–357.
[83] S.A. Sedgewick, D.H. Trevena, Limiting negative pressure of water under dynamic stressing, J. Phys. D: Appl. Phys. 9 (1976) 1983–1990.
[84] P.R. Williams, R.L. Williams, On anomalously low values of the tensile strength of water, Proc. Roy. Soc. London A 456 (2000) 1321–1332.
[85] P.L. Marston, B.T. Unger, Rapid cavitation induced by the reflection of shock waves, in: Y.M. Gupta (Ed.), Proceedings of the Fourth American Physical Society Topical Conference on Shock Waves in Condensed Matter, July 22–25, 1985, Spokane, Washington, Plenum Press, New York, 1986, pp. 401–405.
[86] J.M. Boteler, G.T. Sutherland, Tensile failure of water due to shock wave interactions, J. Appl. Phys. 96 (2004) 6919–6924.
[87] C. Wurster, M. Köhler, R. Pecha, W. Eisenmenger, D. Suhr, U. Irmer, F. Brümmer, D. Hülser, in: J. Herbertz (Ed.), Proceedings of the 1st World Congress on Ultrasonics, Berlin, 1995, Universität Duisburg–Essen, Duisburg, 1995, pp. 635–638, Part 1.
[88] J. Staudenraus, W. Eisenmenger, Fibre-optic probe hydrophone for ultrasonic and shock-wave measurements in water, Ultrasonics 31 (1993) 267–273.
[89] R. Pecha, Private communication.
[90] W.J. Galloway, An experimental study of acoustically induced cavitation in liquids, J. Acoust. Soc. Am. 26 (1954) 849–857.
[91] M. Greenspan, C.E. Tschiegg, Radiation-induced acoustic cavitation apparatus and some results, J. Res. Nat. Bur. Stand. C 71 (1967) 299–312.
[92] E. Herbert, S. Balibar, F. Caupin, Cavitation pressure in water, Phys. Rev. E 74 (2006) 041603 (1–22).
[93] R.D. Finch, Influence of radiation on the cavitation threshold of degassed water, J. Acoust. Soc. Am. 36 (1964) 2287–2292.
[94] W.J. Galloway, Private communication to R.D. Finch, Ref. 6 of Ref. [93].
[95] C.G. Wohl, et al., Review of particle properties, Rev. Mod. Phys. 56 (1984) S1–S299.

[96] J. Winnick, S.J. Cho, *PVT* behavior of water at negative pressures, J. Chem. Phys. 55 (1971) 2092–2097.
[97] J.R. Macdonald, Reconsideration of an experiment on water under negative pressure, J. Chem. Phys. 57 (1972) 3793–3802.
[98] J. Winnick, S.J. Cho, Erratum: *PVT* behavior of water at negative pressures, J. Chem. Phys. 57 (1972) 1018.
[99] H.S. Huang, D.L. Guell, J. Winnick, *PVT* behavior of water at negative pressures: capillary tube deformation effects, J. Chem. Phys. 59 (1973) 6191–6192.
[100] M. Volmer, Über Keimbildung und Keimwirkung als Spezialfälle der heterogenen Katalyse, Z. Elektrochem. 35 (1929) 555–561.
[101] T.J. Jarvis, M.D. Donohue, J.L. Katz, Bubble nucleation mechanisms of liquid droplets superheated in other liquids, J. Colloid Interface Sci. 50 (1975) 359–368.
[102] L. Liebermann, Air bubbles in water, J. Appl. Phys. 28 (1957) 205–211.
[103] P.S. Epstein, M.S. Plesset, On the stability of gas bubbles in liquid–gas solutions, J. Chem. Phys. 18 (1950) 1505–1509.
[104] A.A. Atchley, A. Prosperetti, The crevice model of bubble nucleation, J. Acoust. Soc. Am. 86 (1989) 1065–1084.
[105] E.N. Harvey, A.H. Whiteley, W.D. McElroy, D.C. Pease, D.K. Barnes, Bubble formation in animals, II. Gas nuclei and their distribution in blood and tissues, J. Cell. Comp. Physiol. 24 (1944) 23–34.
[106] F.E. Fox, K.F. Herzfeld, Gas bubbles with organic skin as cavitation nuclei, J. Acoust. Soc. Am. 26 (1954) 984–989.
[107] D.E. Yount, E.Q. Gillary, D.C. Hoffman, A microscopic investigation of bubble formation nuclei, J. Acoust. Soc. Am. 76 (1984) 1511–1521.
[108] N. Bremond, M. Arora, C.-D. Ohl, D. Lohse, Cavitation on surfaces, J. Phys.: Condens. Matter 17 (2005) S3603–S3608.
[109] N. Bremond, M. Arora, C.-D. Ohl, D. Lohse, Controlled multibubble surface cavitation, Phys. Rev. Lett. 96 (2006) 224501 (1–4).
[110] M.T. Tyree, M.H. Zimmermann, Xylem Structure and the Ascent of Sap, second ed., Springer-Verlag, Berlin, Heidelberg, New York, 2002.
[111] H. Cochard, Cavitation in trees, C. R. Physique, this issue, DOI:10.1016/j.crhy.2006.10.012.
[112] M. Versluis, B. Schmitz, A. von der Heydt, D. Lohse, How snapping shrimp snap: through cavitating bubbles, Science 289 (2000) 2114–2117.
[113] S.N. Patek, W.L. Korff, R.L. Caldwell, Deadly strike mechanism of a mantis shrimp, Nature 428 (2004) 819–820.
[114] S.N. Patek, R.L. Caldwell, Extreme impact and cavitation forces of a biological hammer: strike forces of the peacock mantis shrimp Odontodactylus scyllarus, J. Exp. Biol. 208 (2005) 3655–3664.
[115] E.C. Unger, T. Porter, W. Culp, R. Labell, T. Matsunaga, R. Zutshi, Therapeutic applications of lipid-coated microbubbles, Adv. Drug Deliv. Rev. 56 (2004) 1291–1314.
[116] K.M. Balss, C.T. Avedisian, R.E. Cavicchi, M.J. Tarlov, Nanosecond imaging of microboiling behavior on pulsed-heated Au films modified with hydrophilic and hydrophobic self-assembled monolayers, Langmuir 21 (2005) 10459–10467.
[117] C.T. Avedisian, R.E. Cavicchi, M.J. Tarlov, New technique for visualizing microboiling phenomena and its application to water pulse heated by a thin metal film, Rev. Sci. Instrum. 77 (2006), 063706 (1-7).
[118] M.F. Sheridan, K.H. Wohletz, Hydrovolcanism: basic considerations and review, J. Volcano. Geotherm. Res. 17 (1983) 1–29.
[119] T. Kadota, H. Yamasaki, Recent advances in the combustion of water fuel emulsion, Prog. Energy Comb. Sci. 28 (2002) 385–404.
[120] O. Armas, R. Ballesteros, F.J. Martos, J.R. Agudelo, Characterization of light duty Diesel engine pollutant emissions using water-emulsified fuel, Fuel 84 (2005) 1011–1018.
[121] C.-Y. Lin, L.-W. Chen, Engine performance and emission characteristics of three-phase diesel emulsions prepared by an ultrasonic emulsification method, Fuel 85 (2006) 593–600.
[122] M. Nadeem, C. Rangkuti, K. Anuar, M.R.U. Haq, I.B. Tan, S.S. Shah, Diesel engine performance and emission evaluation using emulsified fuels stabilized by conventional and gemini surfactants, Fuel 85 (2006) 2111–2119.
[123] T.J. Mason, J.P. Lorimer, Applied Sonochemistry, Wiley–VCH, Weinheim, 2002.
[124] G. Cravotto, P. Cintas, Power ultrasound in organic synthesis: moving cavitational chemistry from academia to innovative and large–scale applications, Chem. Soc. Rev. 35 (2006) 180–196.
[125] D.G. Shchukin, H. Möhwald, Sonochemical nanosynthesis at the engineered interface of a cavitation microbubble, Phys. Chem. Chem. Phys. 8 (2006) 3496–3506.